Biochemical and Biophysical Research Communications 496 (2018) 1025–1032

Contents lists available at ScienceDirect

Biochemical and Biophysical Research Communications

journal homepage: www.elsevier.com/locate/ybbrc

Homology modeling and docking of AahII-Nanobody complexes reveal the epitope binding site on AahII scorpion toxin

Ayoub Ksouri [a], Kais Ghedira [b], Rahma Ben Abderrazek [a], B.A. Gowri Shankar [c], Alia Benkahla [b], Ozlem Tastan Bishop [d], Balkiss Bouhaouala-Zahar [a, e, *]

[a] Laboratoire des Venins et Molécules Thérapeutiques, Institut Pasteur de Tunis, 13 Place Pasteur, BP74, Tunis Belvédère- University of Tunis El Manar, Tunisia

[b] Laboratory of BioInformatics, Biomathematics and Biostatistics (BIMS), Institut Pasteur de Tunis, 13 Place Pasteur, BP74, Tunis Belvédère- University of Tunis El Manar, Tunis, Tunisia

[c] Laboratory for Venom Peptidomics and Molecular Simulation Bannari Institute of Technology, Alathukombai, Post Sathyamangalam, 638 401, Erode District, Tamil Nadu, India

[d] Research Unit in Bioinformatics (RUBi), Department of Biochemistry and Microbiology, Rhodes University, Grahamstown 6140, South Africa

[e] Faculté de Médecine de Tunis, 15 rue Djebel Lakhdhar, La Rabta, 1007-Université Tunis El Manar, Tunisia

ARTICLE INFO

Article history:
Received 28 December 2017
Accepted 4 January 2018
Available online 31 January 2018

Keywords:
Nanobody
Scorpion toxin
Sequence pattern
Molecular modeling
Molecular docking

ABSTRACT

Scorpion envenoming and its treatment is a public health problem in many parts of the world due to highly toxic venom polypeptides diffusing rapidly within the body of severely envenomed victims. Recently, 38 AahII-specific Nanobody sequences (Nbs) were retrieved from which the performance of NbAahII10 nanobody candidate, to neutralize the most poisonous venom compound namely AahII acting on sodium channels, was established. Herein, structural computational approach is conducted to elucidate the Nb-AahII interactions that support the biological characteristics, using Nb multiple sequence alignment (MSA) followed by modeling and molecular docking investigations (RosettaAntibody, ZDOCK software tools). Sequence and structural analysis showed two dissimilar residues of NbAahII10 CDR1 (Tyr27 and Tyr29) and an inserted polar residue Ser30 that appear to play an important role. Indeed, CDR3 region of NbAahII10 is characterized by a specific Met104 and two negatively charged residues Asp115 and Asp117. Complex dockings reveal that NbAahII17 and NbAahII38 share one common binding site on the surface of the AahII toxin divergent from the NbAahII10 one's. At least, a couple of NbAahII10 – AahII residue interactions (Gln38 – Asn44 and Arg62, His64, respectively) are mainly involved in the toxic AahII binding site. Altogether, this study gives valuable insights in the design and development of next generation of antivenom.

1. Introduction

'Androctonus australis hector' scorpion envenoming is a serious public health problem around the world [1]. Toxicity of the scorpion's venoms is essentially due to the presence of small toxic peptides acting on sodium channels of excitable cells. These toxins belong to two unrelated groups (group I: AahI, AahIII and AahIV and group II (AahII)), distinct in structure and antigenic characteristics [2] [3]. The crystal structure of the most abundant and toxic compound of the Aah venom, referred to as AahII has been previously elucidated and refined [4] [5]. Antibody-based antivenoms are often employed to treat scorpion envenoming. Since the size of the classical antibody exceeds the size of toxin 14-fold, recombinant antibodies against Aah active toxins have been developed to better reach toxicokinetics [6] [7] [8]. Among single domain antibody fragments, we have proposed recombinant Nanobody format (Nb). The VHH encoding Nb is derived from a camel homodimeric HCAb. Hence, we have selected Nbs of 15 kDa displaying Aah toxins' neutralizing capacity (NC) that exceeds previously reported formats [9] [10] [11]. Their corresponding VHH sequences showed subnanomolar affinity (K_D) to Aah toxins (with a K_D ranging from 86 pM to 76 nM as demonstrated by BIAcore experiments) [10]. One

* Corresponding author. Laboratoire des Venins et Molécules Thérapeutiques, Institut Pasteur de Tunis, 13 Place Pasteur, BP74, Tunis Belvédère- Université Tunis El Manar, Tunisia.;

E-mail addresses: balkiss.bouhaouala@pasteur.tn, balkiss.bouhaouala@fmt.utm.tn (B. Bouhaouala-Zahar).

https://doi.org/10.1016/j.bbrc.2018.01.036
0006-291X/

particular Nb referred to as NbAahII10 (0.49 nM K_D) targets a unique epitope on AahII and displays high neutralizing capacity (NC) (estimated to 133 000 LD50 of AahII/mg of Nb or 2000 LD50 per nmol of Nb) [11]. Its humanized format is considered one of the best candidate for the development of a new antivenom [12]. Epitope mapping of Nbs using a real-time SPR approach allowed grouping Nbs according to the epitope complementation for binding AahII, clearly demonstrating that NbAahII10 is the highest effective one [11]. Assuming that NbAahII10 paratope overlaps the AahII 3D surface that interacts with sodium channel, the main purpose was to identify the Nb − AahII toxin interaction surface. We adopted a computational structure analysis strategy based on pharmacological properties related to the affinity (K_D) and the neutralizing capacity (NC) as well as epitope mapping data to determine key residues responsible of optimal toxin neutralization. Generated outcomes highlight the crucial surface directly involved. This achievement gives more valuable insights in the design of next scorpion antivenom.

2. Material and methods

2.1. AahII-specific nanobody sequences analysis and clustering

A total of available 38 VHH (Nbs) sequences were analyzed [11]. These sequences (NbAahII) are specific to *Androctonus Australis hector* scorpion toxin 'AahII′ exhibiting variable affinity and NC. Sequences were clustered according to their primary sequence similarities (special focus on CDR3 parts). Clusters were aligned separately using PROfile Multiple Alignment with predicted Local Structures and three dimensional (3D) constraints “PROMAL3D” [14]. Conserved positions in complementary determining regions (CDRs) were pulled out and specific patterns against AahII were generated. Three sequences were selected for further investigations, and aligned using multiple sequence alignment software (MSA). MSA outputs were visualized, edited and analyzed using 'JALVIEW′ software [15] (Jalview Version 2.9 downloaded and installed on local computer machine).

2.2. Homology modeling

A super workstation computer named “Tesla” with multicore CPU(s) (72 Core) running Debian Linux system (×86/×86_64 Linux/Debian 8.9 “Jessie”) was used (512 Gigabyte of RAM and 12 Tera of storage capacity) for setting high resolution homology models. Rosetta Antibody application [16], specifically designed to work with antibodies, from “ROSETTA 3.8” software package [17] was used as the main tool for Nb structure modeling simulation.

Several templates are chosen from protein database 'PDB' [18]. Each Nb sequence was blasted independently; thereby four templates were selected (three for CDR1, CDR2, and CDR3 and one for framework region FR). Selected templates were assembled then grafted into a unique crude structure, automatically. The final template quality was checked manually in order to validate its suitability for further modeling simulation step. CDR3 part is *de novo* remodeled with a side chains and loop backbones' refinement. The number of generated structures is set to 1000.

Generated model structures are sorted according to 'Rosetta_H3 quality modeling scores'. Top ten model best scores were checked using Ramachandran plot assessment method [19]. Best model was selected then visually double checked (to detect structural anomalies) using the molecular visualization PyMOL software [20].

2.3. Nb - AahII_toxin molecular complex docking

The generated structures of the Nb models were submitted to ZDOCK version 3.0.2 web server [21] and Nb CDR3 region was selected as a targeted pool of binding site residues for filtering output predictions. The crystal structure of AahII toxin (PDB ID: 1PTX) was repaired using RELAX application binary executable from Rosetta package. The entire AahII toxin structure was employed in the molecular docking simulation. Best 10 docking solutions according to the default ZDOCK score were retained for structural assessment. The best energetic pose conformation of the largest cluster of complexes were selected and submitted in GalaxyWEB Web server [22] for complex refinement and repairing. Outputs were visualized and investigated using PYMOL. The retained Nb − AahII toxin complex was characterized. Main amino acid residues involved in Nb − AahII interaction were explored using COCOMAPS (bioCOmplexes COntact MAPS) online server [23]. Intermolecular contact maps of predicted complex structures were illustrated. A maximum distance value is set to 3 Å and 6 Å to report atom-atom interactions within this cut-off limit.

3. Results

A panel of 38 anti AahII Nb binders, previously retrieved from bio-panning of a phage display library, was investigated in primary sequence alignments. Global MSA of the whole Nb sequences was performed as a preliminary test. However, a poor quality MSA alignment was obtained due to a high number of gaps, especially in CDR3 regions, characterized by high variability in length (from 12 to 20 AA) and primary structure (data not shown). To bypass this constraint manual clustering was performed. At least 8 distinct clusters were obtained according to whole sequence homology (Supplementary Fig. 1). As illustrated in Table 1, the conserved positions were selected then pulled out to generate a corresponding general pattern. Three patterns were obtained according to similarity as well as their hydrophobicity (*h*), polarity (o) and residue charge (+, -). The most conserved positions within the CDR1, CDR2 and CDR3 regions are highlighted in bold (Table 1). Independently of the CDR length, the general patterns are as following: **'SGho[(F)*h*](ST)(N)Y(C*h*R)'**, **'I[HN](oP)G(*h*)(T)'** and **'C(A)[+*h*](o)YGYX(W)',** respectively for CDR1 (8-10 residue's length), CDR2 (6-9 residue's length) and CDR3 (12-20 residue's lenghth) regions.

Among the 38 Nb binders', the NbAahII10 sequence distinguished by its very high NC and nanomolar affinity was selected to investigate antibody structural determinants involved in toxin trapping and neutralization. Indeed, two Nb sequences (i.e. NbAahII17 and NbAahII38) belonging to distinct clusters were used as reference (sequence controls), displaying non-significant NC despite their nanomolar affinity. As illustrated in Fig. 1, MSA of the selected Nbs showed significant residue position hyper variability between NbAahII10, NbAahII17 and NbAahII38, in positions 27, 28, 29 and 30 of CDR1. The polar residue Tyr27 in NbAahII10 is substituted by a hydrophobic residue (Val27 and Phe27) in NbAahII17 and NbAahII38, respectively. The second Tyr in position 29 was substituted by the same residues (Val or Phe). Moreover, Phe28 of NbAahII10 is replaced with a Thr28 in the NbAahII17 and NbAahII38 sequences. Interestingly, at position 30 within NbAahII10 the additional polar residue Ser appears to play an important role. The CDR2 regions are hypervariable at all positions. Their sequences differ by > 4 amino acids and no consensus was distinguished. The CDR3 regions are also hypervariable. Nevertheless, the Pro in position 113 is highly conserved between Nb sequence positions and is involved in the CDR3 canonical loop structure. Unexpectedly, we noticed several conserved residues between NbAahII10 and NbAahII17 at five positions: Thr100, Asn103, Gly107, Leu108 and Tyr118. CDR3 region of NbAahII10 is characterized by the presence of special residue distinct Met104 and two negatively charged residues Asp115 and Asp117.

Table 1
Conserved residue positions of the different Nb clusters. The most conserved positions within the CDR1, CDR2 and CDR3 regions are highlighted in bold. Patterns were obtained according to similarity as well as their hydrophobicity (*h*), polarity (*o*) and residue charge (+, -). Most frequent residues in given position are represented between parenthesis (). A or B residues in the same position is marked by two brackets [] and X: hypervariable position.

Nb_AahII	CDR1	CDR2	CDR3
Cluster 1	26 G [(Y)F] (T) X X R [(R)Y] [(R)V] 33	51 I [(Y)I] [PT] G (h) T 58	96 C A [(L)K] [(Q)G] [(S)V] X [(E)S] [TS] Y G Y R G F W Y E (E) X G Y A D W 119
Cluster 2	26 G Y T C T K F N 33	51 I R R D [(S)G] T 57	95 C S [(T)/F] R C [(V)L] T [(S)P} S [(V)L] P Y W 107
Cluster 3	26 G [YD] [SF] Y X S N Y Y 34	52 I N R S G R I T 57	97 C A A G V R T H M P P L A S Y G F D Y W 116
Cluster 4	26 G Y F Y S S N Y C 34	52 I N I A P G R I Y 59	97 C A S T A G N M Y Y G L R G P A D F D Y W 117
Cluster 5	26 G *h* T L [(N)S] [(N)D] Y C 34	51 [FIL] K [SD] [GR] G S (F) T 58	96 C A V T R N S C L G L A K F R P S S Y N Y W 117
Cluster 6	26 G Y T F S N Y R 33	51 I L T D G S T 57	96 C A A G N S R K G Y L R R C G G T D F G Y W 116
Cluster 7	26 G F [STD] F [(S)N] [(I)R] Y [AV] 33	51 I [(M)H] E W [(I)V] P X G[STQ] T 59	97 C A K G V [(Y)L] T [(K)T] Y (V) G (G) A R 111
Cluster 8	26 G F T F S N Y V 33	51 I N H G G G I Q 57	96 C V RA SHYRD Y GP T I Y S W 112
General Pattern	**G *h* o [(F)h] (ST) (N) Y (*Ch*R)**	**I [*h*N] (op) G (*h*) (T)**	**C (A) [+h] (o) Y G Y X (W)**

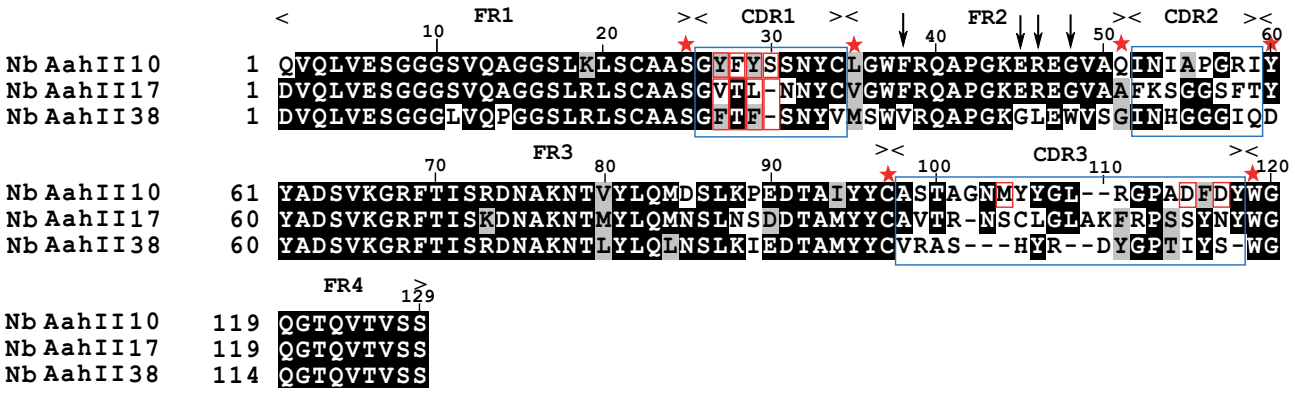

Fig. 1. Primary sequence alignment of specific Nanobody (Nb) anti-AahII scorpion toxin. The 'framework' and 'CDR' regions amino acids numbering are according to IMGT. The CDR regions are boxed in thin blue lines. Hallmark residues in FR2 are marked by vertical arrows. Anchorage residue forming CDRs limits are marked by red stars and Gaps are represented as dashs (-). Residues red boxed in CDR1 shows a clear amino acids substitution in position 27, 28 and 29 with a Serine insertion in position 30. (For interpretation of the references to colour in this figure legend, the reader is referred to the Web version of this article.)

Their 3D structures were simulated and predicted according to the described homology modeling approach. First, homology modeling yielded a distinct grafted structure template for each Nb. Hence, PDB codes 4M5Y, 4B5E and 4RIR were used as templates for NbAahII10 CDR1, CDR2 and CDR3, respectively. The PDB code 3QSK was used as the FR template. All CDR and FR templates were assembled and then relaxed into a common crude template structure. In the case of NbAahII17, the selected and grafted template was shaped from the following PDB codes: 1MVF, 1JTP, 1ZVY and 1MVF (for CDR1, CDR2, CDR3 and FR regions, respectively). The PDB codes 2DQU, 1UCB, 4R90 and 5JMR were used as templates to obtain a common crude template structure (Table 2). Subsequently, the assembled and relaxed templates were used as principal inputs to generate 1000 high quality homology Nb models. 3D structure models were ranked according to Rosetta modeling scores. The highest and lowest scores of the top ten favoured models are reported: (-118/-104.264), (-153.566/-148.044) and (-48.431/-44.529) for NbAahII10, NbAahII17 and NbAahII38, respectively. Quality of the generated structural models was evaluated using Ramachandran plots. As illustrated in Fig. S2 (supplementary data), 99.2% and 0.8% of the NbAahII10 structure residues were in the favoured and allowed regions of the RAMACHANDRAN plots, respectively. Indeed, all residues belonging to NbAahII17 and NbAahII38 structures (100%) were in the RAMACHANDRAN plot favoured region, demonstrating high-quality of the models.

High-resolution homology model is useful for solid structural analysis of surface interactions. Using ZDOCK docking process, we generated the top ten possible binding sites ranked according to an energy-based scoring. The highest ranked complex belongs to the largest cluster (6 of 10 complexes). This complex was further refined to avoid steric clashes tolerated by the rigid-body docking process of ZDOCK (Table 3). Following refinement, the interface contact area increased from 864.4 to 931.3, 757.2 to 903.1 and from 813.3 to 921.3 Å for NbAahII10, NbAahII17 and NbAahII38, respectively. The MolProbity, Clash score, Rotamer outlier and Refinement energy data are reported in Table 3.

In order to assess the residues involved in the molecular interface, we used the COCOMAPS (bioCOmplexes COntact MAPS) web application server. Intermolecular contact maps of complexes are illustrated in Fig. 2. Remarkably, the CDR3 is predicted to dominate the interactions with AahII. NbAahII10 CDR1 region residues (Tyr27, Tyr29, Ser30, Ser31, Tyr33 and Cys34) also interact with AahII toxin. However, CDR1 of NbAahII17 and NbAahII38 are not involved in the interaction with AahII toxin (Fig. 2). Atom-atom interaction was set to a maximum distance value of 3 and 6 Å for CDR3 and CDR1, respectively.

Binding sites (epitopes) in AahII toxin sequence are described as follow: (i) **DDV, C, YFCGR, Y, E, E, K (8-10, 14-18, 21, 24, 25, 28)** and interact with NbAahII17 and NbAahII38, (ii) **WASPYGN (38-44)** discontinuously with **- R (62)** particularly interact with NbAahII10 and (iii) the AahII toxin C-terminal region**, H (64)** common for the three Nbs (Fig. 3).

Residues involved in H bounds as proton donors or acceptors are illustrated in Table 4. Residues contributing to H bond interactions are shown in Fig. 4. Hence, a small number of hydrogen and ionic bond NbAahII10 − AahII interaction, compared to NbAahII17 and NbAahII38.

Table 2
Selected template structures for CDR and FR regions in the first stage of RosettaAntibody homology modeling process.

Nb region	PDB code	Chain	Organism	Template Molecule	Lenght (AA)
NbAahII10 Templates					
VHH FRs	3qsk	B	*Camelus dromedarius*	Anti-RNase A VHH	123
CDR1	4m5y	H	*Homo sapiens*	Fab 5J8 heavy chain	233
CDR2	4b5e	A	*Lama glama*	PS2-8	127
CDR3	4rir	A	*Homo sapiens*	CH58-UA Fab VH	231
NbAahII17 Templates					
VHH FRs	1mvf	A	*Camelus dromedarius*	Camelid VHH	125
CDR1	1mvf	A	*Camelus dromedarius*	Ig 6D9	224
CDR2	1jtp	A	*Camelus dromedarius*	Single-Domain Ab	219
CDR3	1zvy	A	*Camelus dromedarius*	Chimeric hIgG/BR96	229
NbAahII38 Templates					
VHH FRs	5jmr	A	*Camelus dromedarius*	Camelid VHH	125
CDR1	2dqu	H	*Mus musculus*	Ig 6D9	224
CDR2	1ucb	H	*Homo sapiens*	Single-Domain Ab	219
CDR3	4r90	A	*Lama glama*	Chimeric hIgG/Fab BR96	229

Table 3
Parameters and scores of Nb-AahII complexes before (Input) and after (Refined complex) structural refinement, using GalaxyWEB server for protein structure prediction and refinement [22].

Nb-AahII Model	NbAahII10-AahII		NbAahII17-AahII		NbAahII38-AahII	
	Input	Refined complex	Input	Refined complex	Input	Refined complex
Interface area (Å^2)	864,40	931,30	757,20	903,10	813,30	921,30
MolProbity score	2420	1735	2338	1889	2193	1885
Clash score	52,40	17,20	60,30	20,30	41,90	24,90
Rotamer outlier	2.00	0,70	1,30	1,30	1,30	0
Rama favoured (%)	98,90	98,90	98,90	98,90	98,30	98,90
Refinement energy (J/mol)	–	−6654,58	–	−6754,041	–	−6440,996

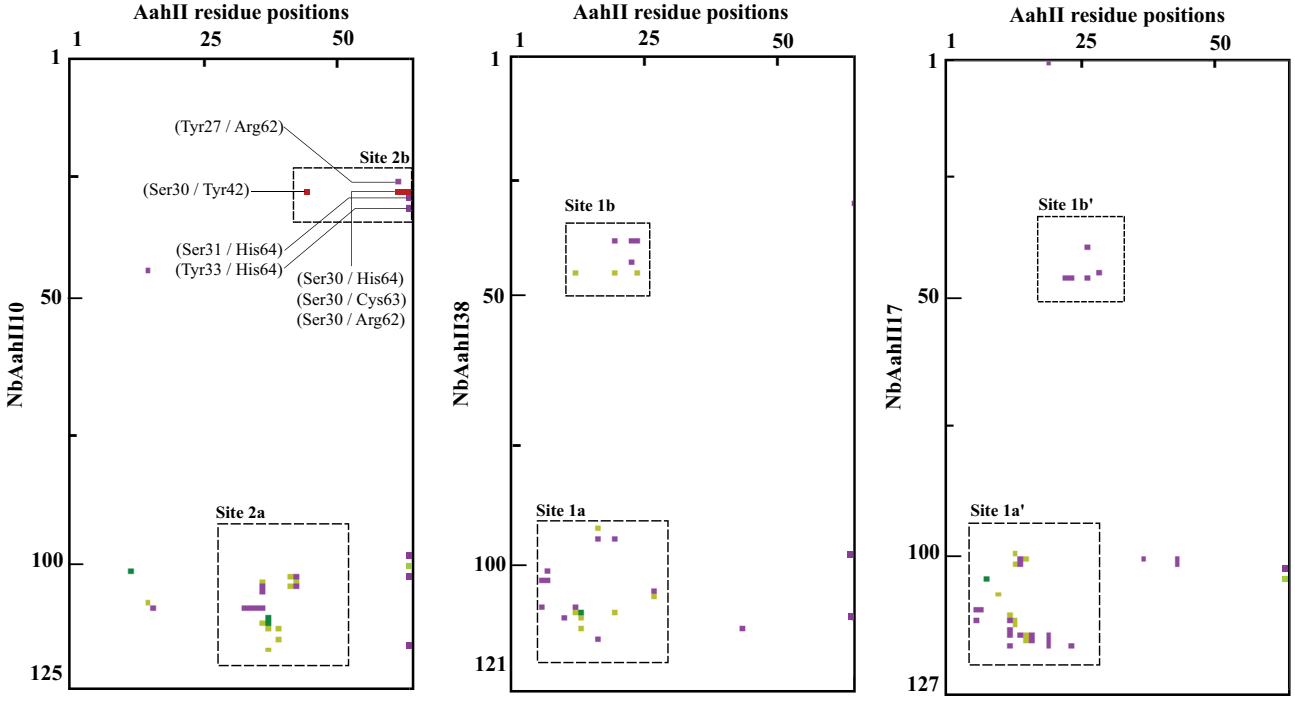

Fig. 2. Contact maps of NbAahII10, NbAahII17 and NbAahII38 against AahII. Yellow, magenta and green dots indicate hydrophobic – hydrophilic, hydrophilic – hydrophilic and hydrophobic – hydrophobic contacts, respectively. Labels highlight the NbAahII10-AahII complex interacting CDR1 residues. In dashed boxes, the NbAahII17/38 common Site 1 (a, b) and NbAahII10 Site 2 (a, b). (For interpretation of the references to colour in this figure legend, the reader is referred to the Web version of this article.)

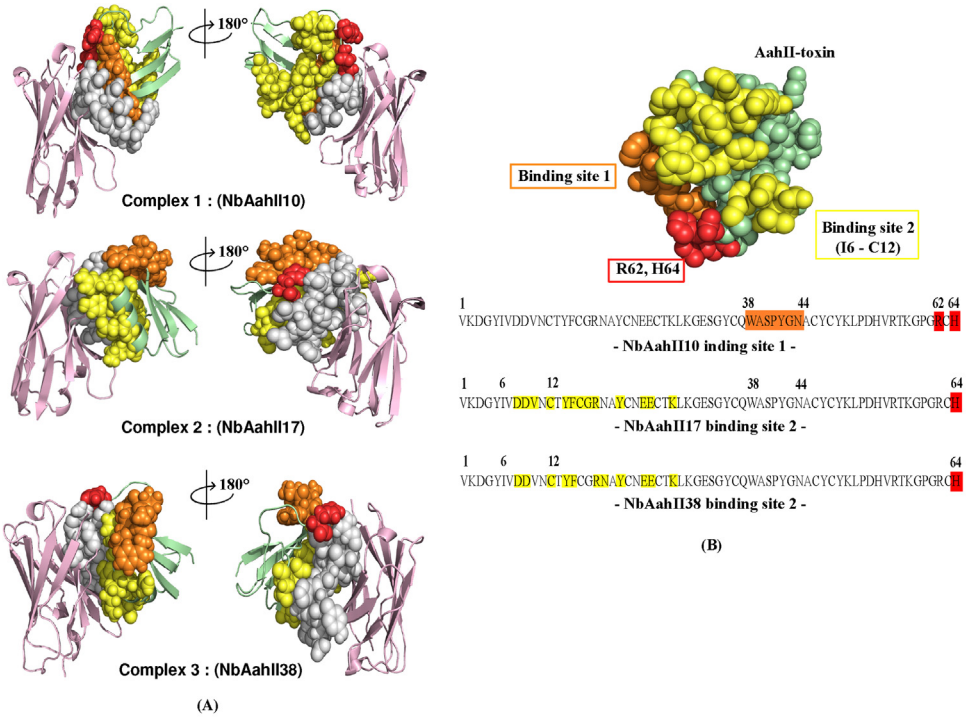

Fig. 3. Binding positions of 3D Nbs structures against AahII. (A) Two faces (rotation of 180°) were represented for NbAahII10 - AahII, NbAahII17 - AahII and NbAahII38 – AahII complexes. Complex structures are shown as coloured cartoon (for Nb and toxin core: light pink and pale green for Nb and AahII toxin, respectively); coloured spheres for binding regions (white for CDR3, yellow for AahII binding site 1, orange AahII binding site 2 and red for AahII C-terminal binding residues). (B) AahII toxin 3D structure and sequence with highlighted binding sites (same colour code). (For interpretation of the references to colour in this figure legend, the reader is referred to the Web version of this article.)

Table 4
List of the intermolecular hydrogen bonds and salt bridges between NbAahII10, NbAahII17 and NbAahII38 binders with AahII scorpion toxin.

Nbs	Chain	Residue number	Residue	Atoms	Chain	Residue number	Residue	Atoms	Distance (Å)
NbAahII10	A	18	ARG	NH1	H	44	GLU	OE1	3,2
	A	18	ARG	NH2	H	44	GLU	OE2	2,78
	A	44	ASN	ND2	H	103	MET	O	2,75
	H	112	ASP	N	A	39	ALA	O	2,82
NbAahII17	A	18	ARG	NE	H	1	ASP	OD2	2,89
	H	3	GLN	NE2	A	21	TYR	OH	3,06
	A	28	LYS	NZ	H	39	GLN	OE1	2,84
	H	45	ARG	NH1	A	24	GLU	OE1	2,96
	H	45	ARG	NH1	A	25	GLU	OE2	2,82
	H	45	ARG	NH2	A	24	GLU	OE1	2,87
	H	100	ARG	NH2	A	16	CYS	O	3,1
	H	101	ASN	ND2	A	16	CYS	O	3,06
	H	104	LEU	N	A	64	HIS	O	2,86
	A	15	PHE	N	H	112	SER	O	2,85
	A	14	TYR	OH	H	115	ASN	OD1	3,3
	A	21	TYR	OH	H	117	TRP	O	3,08
	H	117	TRP	NE1	A	14	TYR	OH	3,03
NbAahII38	H	45	LEU	N	A	25	GLU	OE2	2,92
	A	18	ARG	NH1	H	95	TYR	OH	2,85
	H	98	ARG	NH2	A	64	HIS	NE2	2,93
	A	15	PHE	N	H	109	ILE	O	2,87
	H	110	TYR	OH	A	64	HIS	ND1	2,99
	A	64	HIS	ND1	H	110	TYR	OH	2,99

4. Discussion

Following our computational approach, AahII specific Nb sequences were investigated at structural level in order to better understand elements responsible of specificity as well as toxicity to AahII, thereby throughout the full meaning analysis of divergence in primary Nb sequences. First, a MSA has been assessed for evaluating divergent and common features connecting sequence and function [24]. No standard method applicable for all conditions exists. It is therefore important to optimize alignment method because output alignment inspection, interpretation and manual adjustment are required to generate the alignment that best gives insight into the biological of the sequences [25] [15]. Data from MSA analysis allow the assignement of general patterns of CDRs, often

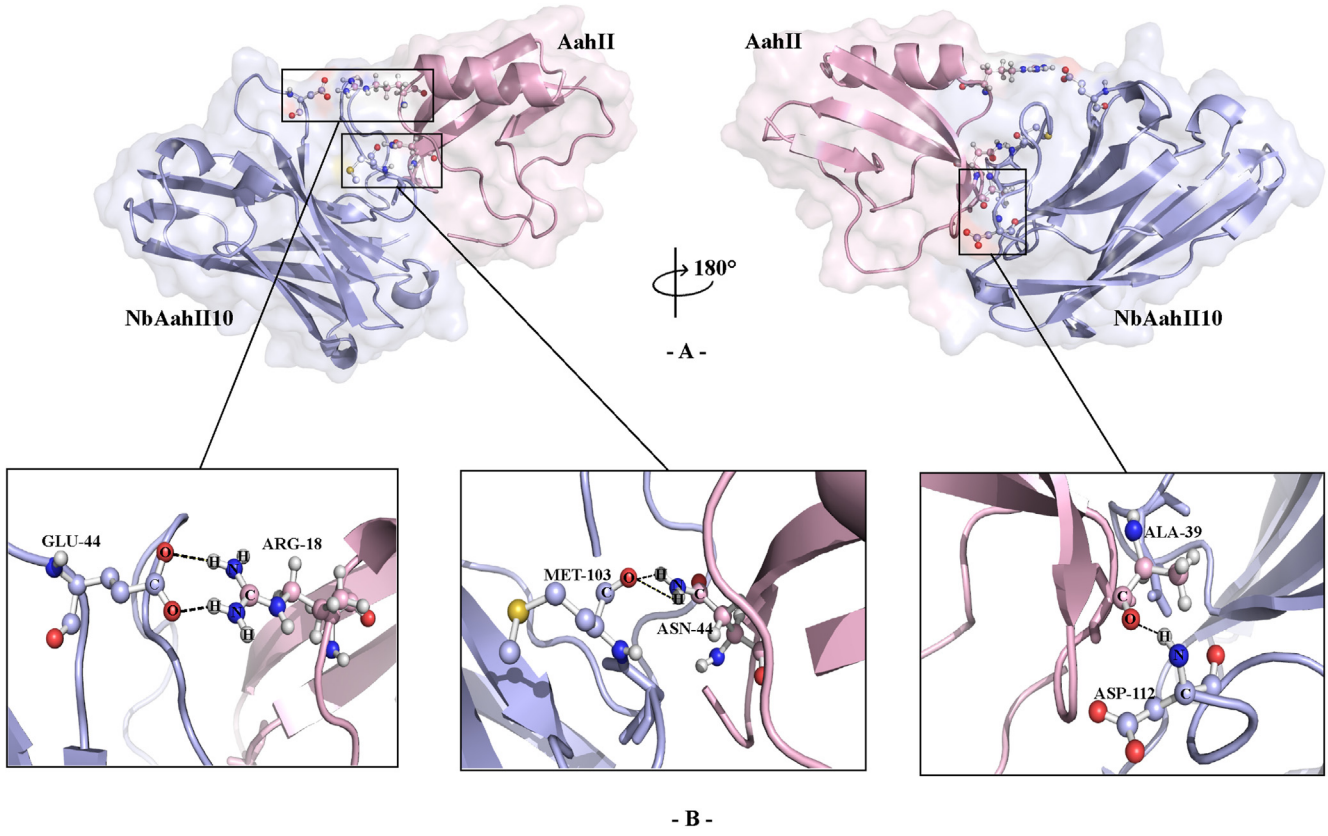

Fig. 4. 3D structure of NbAahII10 – AahII complex (Colours are light blue and light pink for NbAahII10 and AahII toxin, respectively), on two faces (rotation of 180°). Residues Glu44-Arg18, Met103-Asn44 and Asp112-Ala39 were the residues forming HH bound. Residues predicted to be crucial for complex stability are highlighted in sticks and interactions are represented by dashed black lines. (For interpretation of the references to colour in this figure legend, the reader is referred to the Web version of this article.)

assumed to account for the antigen recognition and binding site [26]. Selected sequences were analyzed by investigating crucial residues/signature involved that may supports the previously demonstrated specificity [11].

Considering the NbAahII10, NbAahII17 and NbAahII38, MSA highlights crucial positions in CDRs. Two polar residues as amino acid sequence differences on the NbAahII10 CDR1 region (Tyr27 and Tyr29) appear to play an important role. Those positions are dissimilar from the analogous hydrophobic residues (in same 27 and 29 positions) in NbAahII17 and NbAahII38 normally buried inside the protein core. In addition, the same MSA indicates in position 30 an inserted polar residue Ser30 that belongs to NbAahII10 sequence. Altogether, polar residues may affect physiochemical traits of CDR1 and possibly involved in the NbAahII10 high biological activity. The CDR2 and CDR3 hyper variability in sequences cannot leads to clear signature. Therefore, structural computational approach is required to further elucidate the NbAahII interactions that support the demonstrated biological traits.

Homology modeling, can be an alternative strategy to test hypotheses related to structure-function relationships [27]. With the limited number of antibody structures in PDB [28], we used specific homology modeling 3D simulations to design and predict Nb' models. The existing homology modeling servers do not provide high resolution refinement of antibody structures and do not consider thermodynamics during modeling [28]. Interestingly, RosettaAntibody software (that uses 4 template structures assembled in one crude template) is more suitable to obtain predict structure models. Since CDR3 loop modeling is the most critical stage, it can be only remodeled "de novo" to better fit the high variability in length and sequence with the absence of a canonical structure [29].

As expected, models generated by the RosettaAntibody software tool were assessed as high-quality 3D structure models with a total number of residues located in favoured regions in the Ramachadran plots, for the three simulated models (supplementary, Fig. 2).

Thereafter, molecular docking investigations on the three models against the crystal structure of AahII toxin revealed the presence of two distinct major antigenic sites on the AahII surface. NbAahII17 and NbAahII38 share one common binding site totally different from the NbAahII10 one's. Those outcomes are in overall good agreement with experimental mapping data previously reported [11]. Furthermore, consistent with our outcomes, Fab4C1 neutralizing AahII experimental structure complex shows discontinuous AahII epitope, essentially involving C-terminal region [30], which is part of the six antigenic groups previously described [31]. In the present work, two positions are mainly overlapped and in full accordance with the generated binding site of "best in class" NbAahII10 (Gln38 – Asn44) and (Arg62 – His64). As well, NbAahII17 and NbAahII38 binding sites overlapped with two regions via distinct residues (Asp8 – Val10, Lys28).

The NbAahII10, with the entirely distinct binding site suggests that its AahII trapping involves either a distinct toxin attachment 3D orientation. Interestingly, we showed that the AahII (Trp38 – Asn44) segment interacts mainly with the NbAahII10 CDR3 through several residues. Only Met103 and Asp112 are making H bound interactions with AahII Asn44 and Ala39, respectively. Exceptionally, AahII Trp38 exhibits various potent interactions with Met103, Arg108, Tyr105 and Ala111 of the NbAahII10 CDR3. This

result confirms the previous demonstration, across chemical assessment, that Gln37 – Asn44 loop is mainly involved in the scorpion α-toxins mode of action [32] and segment Ala39 – Ala45 has been identified as a main region responsible for antigenic reactivity [33]. Likewise, the individual residues Trp38 has been described playing an important role in bioactivity [34]. More recently, Trp38 and Asn44 at the side of the toxin core were cited as recognizing the domain IV voltage-sensing module of the sodium channel [35]. Herein, we showed that the NbAahII10 also bind same residue positions and therefore may block the AahII surface directly interacting with the domain IV of the sodium channels.

Several studied demonstrated that C-terminal region of AahII toxin is often belonging to the antigenic and active site mainly involved in interaction with antibodies [32,34].

Indeed, AahII C-terminal His64 is involved in all Nbs – AahII complexes of interaction and AahII Arg62 interacts with only NbAahII10 CDR1 and participate to the binding capacity [35].

In conclusion, NbAahII10 differs by pertinent variations within CDR1 that seem to be crucial in AahII neutralization [34]. Indeed, AahII Trp38 make various interactions the NbAahII10 CDR3. Altogether, this study gives valuable insights in the design and development of next generation of antivenom (NGA) for targeting specific scorpion toxins.

Conflicts of interest

Author declare No conflict of Interest.

Funding

This work was supported in parts by the H3Africa Bioinformatics Network (H3ABioNet) and in parts by INT/Tunisia/P-06/2013 Tunisia-India bilateral project.

Acknowledgements

Thanks, are addressed to Professor Hechmi Louzir, General Director of Institut Pasteur, Dr Mohamed El Ayeb, Founder of LVT Lab and to Dr Riadh Kharrat, Director of LVMT Research Lab for their constant encouragements.

The authors are grateful to Professor Rembert Pieper who helped correcting the English version.

Appendix A. Supplementary data

Supplementary data related to this article can be found at https://doi.org/10.1016/j.bbrc.2018.01.036.

References

[1] M. Bouaziz, M. Bahloul, H. Kallel, M. Samet, H. Ksibi, H. Dammak, M.N.B. Ahmed, K. Chtara, H. Chelly, C.B. Hamida, N. Rekik, Epidemiological, clinical characteristics and outcome of severe scorpion envenomation in South Tunisia: multivariate analysis of 951 cases, Toxicon 52 (2008) 918–926, https://doi.org/10.1016/j.toxicon.2008.09.004.

[2] M. el Ayeb, E.M. Bahraoui, C. Granier, H. Rochat, Use of antibodies specific to defined regions of scorpion alpha-toxin to study its interaction with its receptor site on the sodium channel, Biochemistry (Mosc.) 25 (1986) 6671–6678.

[3] Polymorphism and quantitative variations of toxins in the venom of the scorpion Androctonus australis Hector - ScienceDirect, (n.d.). https://www.sciencedirect.com/science/article/pii/0041010185900054 (accessed December 18, 2017).

[4] J.C. Fontecilla-Camps, C. Habersetzer-Rochat, H. Rochat, Orthorhombic crystals and three-dimensional structure of the potent toxin II from the scorpion androctonus australis hector, Proc. Natl. Acad. Sci. U. S. A 85 (1988) 7443–7447.

[5] C. Devaux, B. Jouirou, M. Naceur Krifi, O. Clot-Faybesse, M. El Ayeb, H. Rochat, Quantitative variability in the biodistribution and in toxinokinetic studies of the three main alpha toxins from the Androctonus australis hector scorpion venom, Toxicon Off. J. Int. Soc. Toxinology 43 (2004) 661–669, https://doi.org/10.1016/j.toxicon.2004.02.021.

[6] C. Devaux, E. Moreau, M. Goyffon, H. Rochat, P. Billiald, Construction and functional evaluation of a single-chain antibody fragment that neutralizes toxin AahI from the venom of the scorpion Androctonus australis hector, Eur. J. Biochem. 268 (2001) 694–702.

[7] M. Juste, M.F. Martin-Eauclaire, C. Devaux, P. Billiald, N. Aubrey, Using a recombinant bispecific antibody to block Na+ -channel toxins protects against experimental scorpion envenoming, Cell. Mol. Life Sci. CMLS 64 (2007) 206–218, https://doi.org/10.1007/s00018-006-6401-3.

[8] M. Mousli, C. Devaux, H. Rochat, M. Goyffon, P. Billiald, A recombinant single-chain antibody fragment that neutralizes toxin II from the venom of the scorpion Androctonus australis hector, FEBS Lett. 442 (1999) 183–188.

[9] I. Hmila, B.A.-B. Abdallah R, D. Saerens, Z. Benlasfar, K. Conrath, M.E. Ayeb, S. Muyldermans, B. Bouhaouala-Zahar, VHH, bivalent domains and chimeric Heavy chain-only antibodies with high neutralizing efficacy for scorpion toxin AahI', Mol. Immunol. 45 (2008) 3847–3856, https://doi.org/10.1016/j.molimm.2008.04.011.

[10] I. Hmila, D. Saerens, R. Ben Abderrazek, C. Vincke, N. Abidi, Z. Benlasfar, J. Govaert, M. El Ayeb, B. Bouhaouala-Zahar, S. Muyldermans, A bispecific nanobody to provide full protection against lethal scorpion envenoming, FASEB J. Off. Publ. Fed. Am. Soc. Exp. Biol. 24 (2010) 3479–3489, https://doi.org/10.1096/fj.09-148213.

[11] R.B. Abderrazek, I. Hmila, C. Vincke, Z. Benlasfar, M. Pellis, H. Dabbek, D. Saerens, M. El Ayeb, S. Muyldermans, B. Bouhaouala-Zahar, Identification of potent nanobodies to neutralize the most poisonous polypeptide from scorpion venom, Biochem. J. 424 (2009) 263–272, https://doi.org/10.1042/BJ20090697.

[12] R. Ben Abderrazek, C. Vincke, I. Hmila, D. Saerens, N. Abidi, M. El Ayeb, S. Muyldermans, B. Bouhaouala-Zahar, Development of Cys38 knock-out and humanized version of NbAahII10 nanobody with improved neutralization of AahII scorpion toxin, Protein Eng. Des. Sel. PEDS 24 (2011) 727–735, https://doi.org/10.1093/protein/gzr037.

[14] J. Pei, B.-H. Kim, N.V. Grishin, PROMALS3D: a tool for multiple protein sequence and structure alignments, Nucleic Acids Res. 36 (2008) 2295–2300, https://doi.org/10.1093/nar/gkn072.

[15] A.M. Waterhouse, J.B. Procter, D.M.A. Martin, M. Clamp, G.J. Barton, Jalview Version 2—a multiple sequence alignment editor and analysis workbench, Bioinformatics 25 (2009) 1189–1191, https://doi.org/10.1093/bioinformatics/btp033.

[16] B.D. Weitzner, J.R. Jeliazkov, S. Lyskov, N. Marze, D. Kuroda, R. Frick, J. Adolf-Bryfogle, N. Biswas, R.L. Dunbrack, J.J. Gray, Modeling and docking of antibody structures with Rosetta, Nat. Protoc. 12 (2017) 401–416, https://doi.org/10.1038/nprot.2016.180.

[17] License and Download | RosettaCommons, (n.d.). https://www.rosettacommons.org/software/license-and-download (accessed December 18, 2017).

[18] H.M. Berman, J. Westbrook, Z. Feng, G. Gilliland, T.N. Bhat, H. Weissig, I.N. Shindyalov, P.E. Bourne, The protein data bank, Nucleic Acids Res. 28 (2000) 235–242.

[19] RAMPAGE: Ramachandran Plot Assessment, (n.d.). http://mordred.bioc.cam.ac.uk/~rapper/rampage.php (accessed December 18, 2017).

[20] L.L.C. Schrödinger, The PyMOL Molecular Graphics System, Version 1.8, 2015.

[21] B.G. Pierce, K. Wiehe, H. Hwang, B.-H. Kim, T. Vreven, Z. Weng, ZDOCK server: interactive docking prediction of protein–protein complexes and symmetric multimers, Bioinformatics 30 (2014) 1771–1773, https://doi.org/10.1093/bioinformatics/btu097.

[22] J. Ko, H. Park, L. Heo, C. Seok, GalaxyWEB server for protein structure prediction and refinement, Nucleic Acids Res. 40 (2012) W294–W297, https://doi.org/10.1093/nar/gks493.

[23] A. Vangone, R. Spinelli, V. Scarano, L. Cavallo, R. Oliva, COCOMAPS: a web application to analyze and visualize contacts at the interface of biomolecular complexes, Bioinforma. Oxf. Engl 27 (2011) 2915–2916, https://doi.org/10.1093/bioinformatics/btr484.

[24] G. Raghava, S.M. Searle, P.C. Audley, J.D. Barber, G.J. Barton, OXBench: a benchmark for evaluation of protein multiple sequence alignment accuracy, BMC Bioinf. 4 (2003) 47, https://doi.org/10.1186/1471-2105-4-47.

[25] G. Blackshields, I.M. Wallace, M. Larkin, D.G. Higgins, Analysis and comparison of benchmarks for multiple sequence alignment, Silico Biol. 6 (2006) 321–339.

[26] V. Kunik, B. Peters, Y. Ofran, Structural consensus among antibodies defines the antigen binding site, PLoS Comput. Biol. 8 (2012), https://doi.org/10.1371/journal.pcbi.1002388.

[27] Z. Xiang, Advances in homology protein structure modeling, Curr. Protein Pept. Sci. 7 (2006) 217–227.

[28] A. Sircar, K.A. Sanni, J. Shi, J.J. Gray, Analysis and modeling of the variable region of camelid single domain antibodies, J. Immunol. Baltim. Md 1950 (186) (2011) 6357–6367, https://doi.org/10.4049/jimmunol.1100116.

[29] B.D. Weitzner, J.R. Jeliazkov, S. Lyskov, N. Marze, D. Kuroda, R. Frick, J. Adolf-Bryfogle, N. Biswas, R.L. Dunbrack, J.J. Gray, Modeling and docking of antibody structures with Rosetta, Nat. Protoc. 12 (2017) 401–416, https://doi.org/10.1038/nprot.2016.180.

[30] E. Bahraoui, J. Pichon, J.M. Muller, H. Darbon, M. Elayeb, C. Granier, J. Marvaldi, H. Rochat, Monoclonal antibodies to scorpion toxins. Characterization and

molecular mechanisms of neutralization, J. Immunol. Baltim. Md 1950 (141) (1988) 214–220.
[31] C. Devaux, M. Juin, P. Mansuelle, C. Granier, Fine molecular analysis of the antigenicity of the Androctonus australis hector scorpion neurotoxin II: a new antigenic epitope disclosed by the pepscan method, Mol. Immunol. 30 (1993) 1061–1068, https://doi.org/10.1016/0161-5890(93)90152-2.
[32] R. Kharrat, H. Darbon, H. Rochat, C. Granier, Structure/activity relationships of scorpion α-toxins, Eur. J. Biochem. 181 (1989) 381–390, https://doi.org/10.1111/j.1432-1033.1989.tb14735.x.
[33] M. Gur, R. Kahn, I. Karbat, N. Regev, J. Wang, W.A. Catterall, D. Gordon, M. Gurevitz, Elucidation of the molecular basis of selective recognition uncovers the interaction site for the core domain of scorpion α-toxins on sodium channels, J. Biol. Chem. 286 (2011) 35209–35217, https://doi.org/10.1074/jbc.M111.259507.
[34] I.P. Fabrichny, G. Mondielli, S. Conrod, M.-F. Martin-Eauclaire, Y. Bourne, P. Marchot, Structural insights into antibody sequestering and neutralizing of Na+ channel α-type modulator from old world scorpion venom, J. Biol. Chem. 287 (2012) 14136–14148, https://doi.org/10.1074/jbc.M111.315382.
[35] F. Bosmans, J. Tytgat, Voltage-gated sodium channel modulation by scorpion α-toxins, Toxicon off, J. Int. Soc. Toxinology 49 (2007) 142–158, https://doi.org/10.1016/j.toxicon.2006.09.023.